THE PENNSYLVANIA STATE UNIVERSITY
SCHREYER HONORS COLLEGE

ENGINEERING SCIENCE AND MECHANICS DEPARTMENT

THE DESIGN OF A MULTI-SENSING FLEXIBLE SYSTEM USED FOR REAL-TIME MONITORING

JUNGHSIEN WEI
SPRING 2019

A thesis
submitted in partial fulfillment
of the requirements
for a baccalaureate degree
in Engineering Science
with honors in Engineering Science

Reviewed and approved* by the following:

Huanyu Cheng
Assistant Professor of Engineering Science and Mechanics Thesis Supervisor

Judith Todd
Professor of Engineering Science and Mechanics Honors Advisor

Judith Todd
Department Head
P. B. Breneman Chair and Professor of Engineering Science and Mechanics

* Signatures are on file in the Schreyer Honors College.

ABSTRACT

Recently, massive data generated by wearable and flexible electronics set demand for efficient communication between sensors and terminals. High speed, low power consumption, and small hardware size are the key factors in data communication. As an example, we have demonstrated an integrated sensing system, including the power supply unit, sensors for collecting data, data processing (the filter and magnifier) and a communication module. The communication module is based on the low-power Bluetooth technology. Fast and reliable data collection is achieved, which is confirmed by the comparison with a wired processing module. We aim to expand our design to multi-sensing (such as strain, temperature, and pH) and physiological monitoring based on flexible and wearable electronics.

TABLE OF CONTENTS

LIST OF FIGURES iii

LIST OF TABLES iv

ACKNOWLEDGEMENTS v

Chapter 1 .... -
    Background & Introduction 1

    1.1 Literature review 1
    1.2 Principle 7
        1.2.1 Instrument amplifier 7
        1.2.2 High pass filter 7
        1.2.3 Lowpass filter 8
        1.2.4 Operational amplifier 9
        1.2.5 Notch filter 9
    1.3 Introduction 10

Chapter 2 .... -
    Methodology 11

    2.1 Design plan & equipment used 11
        2.1.1 Customer needs 11
        2.1.2 Engineering requirement 12
    2.2 Methods 13

Chapter 3 .... -
    Testing Progress & Results 14

Chapter 4 .... -
    Discussion 29

Chapter 5 .... -
    Conclusion 31

Appendix A Keil code for Bluetooth 32

Appendix B Components list 34

BIBLIOGRAPHY 35

LIST OF FIGURES

Figure 1. Embedded platform powered by the solar harvester. [3]..3

Figure 2. RF waves convert into energy power. [7]..3

Figure 3. The structure of ECG signal. [9] 4

Figure 4. GAP roles of peripheral and central. [17]...6

Figure 5. Instrument amplifier. [12]...7

Figure 6. 1st Order High Pass Filter. [13]..8

Figure 7. 1st Order Low Pass Filter. [14] 8

Figure 8. Operational amplifier. [15]...9

Figure 9. Notch Filter. [16]...9

Figure 10. ECG sensor output simulation...15

Figure 11. Circuit of the ECG sensor simulation..15

Figure 12. The circuit of ECG sensor. 16

Figure 13. High-pass filter bode diagram. 17

Figure 14. Low-pass filter bode diagram..18

Figure 15. Notch filter bode diagram..19

Figure 16. ECG testing. 20

Figure 17. ECG diagram from bio amplifier sensor (top) and our own ECG sensor (bottom). 20

Figure 18. Own design ECG diagram...21

Figure 19. Data zoom in at the red circle..21

Figure 20. Bio amplifier ECG diagram...22

Figure 21. Data zoom in at the blue circle. 22

Figure 22. Comparison of both ECG diagram in origin scale...23

Figure 23. Comparison of both ECG diagram in adjustment scale of 10.3. 23

Figure 24. Comparison of both ECG waves in a second. 24

Figure 25. Bluetooth chip (nrf51822). 24

Figure 26. ECG signal data from mobile application. 25

Figure 27. Bluetooth screen. 27

Figure 28. Block diagram of the device. 28

Figure 29. Speed limit for different operating system. [21]...30

LIST OF TABLES

Table 1: A priority-ranked list of customer needs. 11

Table 2: A “Translated” list of engineering requirement. 12

Table 3. Voltage measurement from Bluetooth and Oscilloscope. 25

ACKNOWLEDGMENTS

I can't be thankful enough to acknowledge all parties that supported my research. I believe this is not something that can be done alone by myself. It is my great honor to receive guidance from the professors and help from the graduate students, which resulted in the completion of this thesis.

I wish to express my sincere thanks to Dr. Todd, the head of the engineering science and mechanic department and my academic advisor, for providing me with all the necessary facilities for the research and giving all scholarly advice and scientific approach.

I am also grateful to Dr. Cheng, my thesis supervisor and assistant professor in the Department of engineering science and mechanics. I am extremely thankful and indebted to him for sharing expertise, his valuable guidance and encouragement.

I thank profusely to the graduate students, Jia Zhu, and Ning Yi, in Dr.Cheng's lab for their prompt inspiration and timely suggestions to enable me to complete my thesis.

I also thank my parents and friends for accompanying me to acquire rewarding achievements, and for giving me uninterrupted support as well as continuous encouragement during my research pursuit.

Chapter 1 -Background & Introduction

1.1 Literature review

Flexible electronics have the characteristics of high wiring density, lightweight, thin thickness, and high bending property. The technique could be used for healthcare systems and human machine interfaces. However, current stretchable configurations were constrained to single-layer designs due to limited material processing capabilities in soft electronic systems. [1] Hence, we aimed to combine multiple chips into one or two chips and integrate the existing components into multiple layers in order to implement multiple functions of the system. We would focus on exploring the power supply of the circuit, and electrophysiological sensor (ECG sensor).

There were different types of power source for the embedded system, and energy harvesting technologies were one of them. Energy harvesting technology converted small amounts of ambient energy into usable electrical energy. It allowed the embedded system to operate where there was no conventional power source. Energy harvesting technology could generally be divided into five areas, which were solar, magnetic, vibration (piezoelectric), thermoelectric, and radio frequency (RF). [2] Solar energy was a renewable and sustainable form of energy. We could use several solar panels and photovoltaic (PV) harvesting circuits to operate the system. However, there were several issues to tackle for small and low-power embedded devices with solar harvesting system. For example, the power consumption was higher than the amount of the output power, which was not able to apply MPPT (maximum-power-point tracking) implementation. Besides, it was not always feasible separating the embedded systems from solar harvester because the scavenger circuit and the power device would interact with each other. [3] Recently, scientists have provided a new solution to improve the efficiency of solar energy harvester by shrinking the size of PV modules and reducing the capacity of the energy reservoir. A step-up voltage regulator (LTC3401), which was shown in Figure 1, could provide a stable 3.3 V for an embedded system with up to 97% efficiency. [3] Magnetic induction could be generated by small vibrations of magnets wobbling on a cantilever due to Faraday's law of induction. Based on the theory, researchers had investigated in ferrofluid for electromagnetic ferrofluid-based energy harvesters. Ferrofluids, unlike solid magnet, could easily change its shapes and respond to very small acceleration levels. It offers unique capabilities to design scalable energy harvesters. Currently, the ferrofluids energy harvesting system could provide an output power of around 80 mW/g by harvesting 2.2 Hz low frequency. [4] For piezoelectric energy harvester, it could convert small mechanical strain into voltage, such as low-frequency vibrations, human motion, and acoustic noise. The primary challenge of a piezo harvester was the acquirement of efficiency by matching the resonance frequency to driving frequency. As a result, scientists have used human body-based piezoelectric harvesters to generate the voltage and supply the power. The results of the experiment of the PE harvester showed that the maximum voltage was 7.68 V at 7mi/h. [5] The technique could be potentially used on autonomous operation applications on human body. Next, due to the theory of the Seebeck and Peltier effects, the voltage could be produced by a temperature difference between two dissimilar conductors and used to develop a heater or cooler by running an electric current through two dissimilar junctions. However, thermoelectric devices that had lower conversion efficiency and relatively higher cost were limited to high-value applications. Therefore, scientists tried to find a solution by using different thermoelectric materials to improve the efficiency and lower the cost. Recently, researchers have harvested energy by using flexible thermoelectric generators on the human body. Although the voltage of the open circuit and the power output were 22.1 mV and 2.21 nW for a prototype ($5 \times 5 \times 2.5$ mm^3) [6], which was too low for being a power source, it had huge potential for being the source of a healthcare sensor on the human body. Radio frequency (RF) was an abundant source for energy harvesting. Because of the difference of potential energy, the energy could be captured by RF-to-DC integrated circuit from the movement charge carriers, which was shown in Figure 2, but the circuit did require proximity to a transmitting antenna. [7] For example, STMicroelectronics has launched a new NFC chip, M24LR16E, which was able to harvest energy by converting ambient radio waves into a voltage output. The output voltage was between 1.7 V and 2.3 V. [8]

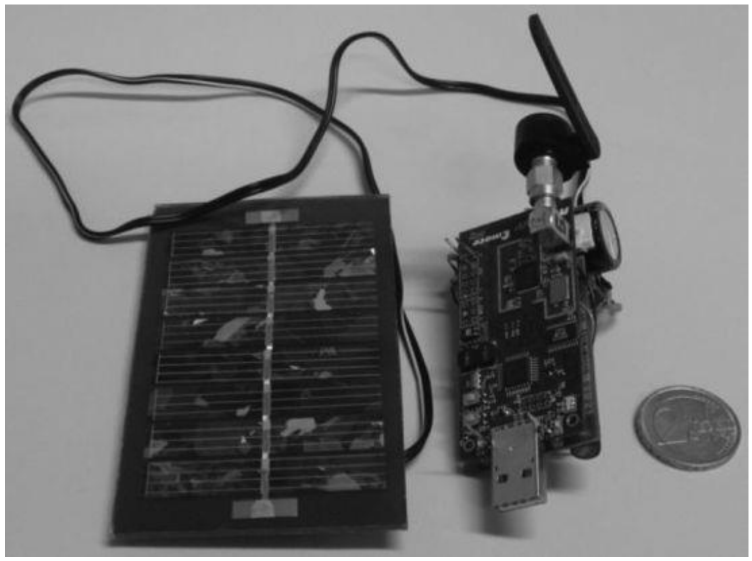

Figure 1. Embedded platform powered by the solar harvester. [3]

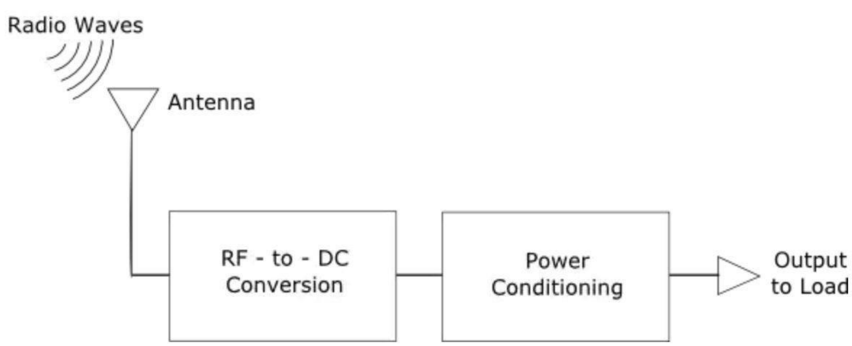

Figure 2. RF waves convert into energy power. [7]

The electrophysiological (ECG) signal was weak, and it was easily influenced by surrounding noise. Therefore, we must first have the basic knowledge of intracellular potential as well as body surface potential so as to further understand the ECG and design the sensor. When the cardiomyocytes (cardiac muscle cell) started depolarizing, the permeability of the cell membrane to sodium ion would change rapidly. Hence, large amounts of sodium ion of lower permeability would enter into the cell, which made the inside become positive potential (about 20 mV) in order to produce slow inward current. This progress was called the 0th stage. Besides, there were three stages after depolarization. The potential would slowly return to the stationary point, and it was able to repolarize. The first stage was that the potential voltage would change from +20 mV to 0 mV because the sodium channel closed quickly. Then, Ca2+ would slowly enter the cell and produce a slow internal current in stage 2. Last, a sodium-potassium pump mechanism on the cell membrane would discharge Na+ and increase the concentration of K+, which made the potential drop back to MRP (Membrane Resting Potential). Therefore, when our heart started pumping, there would be voltage produced, which was often called electrophysiological. The P wave was the first ECG signal from the atria. Then a physiological signal would occur with a delay because the electrical depolarization, and after proceeding into the ventricles, there was the greatest value of the ECG signal, which was known as the QRS complex. The reason was that the muscle mass in the ventricles was greater than others. Moreover, there was the ST segment and the T wave which represented the reflecting repolarization of the myocardium. The completed structure of ECG signal wave was displayed in Figure 3.

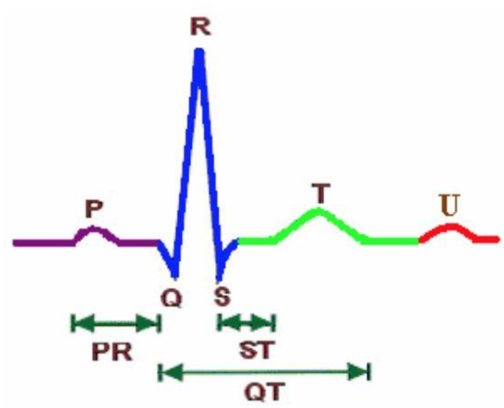

Figure 3. The structure of ECG signal. [9]

For the purpose of measuring the ECG signal, a Dutch physiologist, Willem Einthoven, invented the first practical electrocardiogram in 1903 [11]. He introduced vectors into electrocardiography. In Einthoven's theory, he made the heart as the middle of the triangle at any moment in order to achieve the total vector on three axes plan as zero. Therefore, we could apply the equation to plot the ECG diagram.

There were many kinds of ECG lead measurements nowadays, but twelve leads measurement was the most commonly used for analysis. When designing a hardware ECG sensor, we should understand that ECG signal was very low in amplitude (1μV~1mV) and noisy. Besides, the skin impedance was between 10kΩ and 200kΩ [9] Hence, using an operational amplifier with 10MΩ or more input impedances would easily make the input signal enter the amplifier. Moreover, attaching a high pass filter with certain cut-off frequency could remove the noise from the battery effect of the electrodes and human body, and a low pass filter could isolate the noise at high frequency. [10] Furthermore, the most external noise was the AC power supplied at 60Hz. To eliminate interference noise, there were two solutions. One was driven-right-leg (DRL) circuit. The circuit could minimize the common voltage, which represented a lower impedance path between the human and the amplifier. Also, if there was leakage current, the device would make leakage current flow to the ground through the auxiliary operational amplifier, which was an electrical safety consideration. The second solution was to insert a notch filter in the circuit to further remove a particular frequency. Therefore, designing a wearable ECG device was feasible, and it could become a low-cost and comfortable instrument in the future. Moreover, we would like to combine the circuit with Bluetooth 4.0. Bluetooth 4.0, Bluetooth low energy (BLE) had the same feature as classic Bluetooth. It could be used for exchanging data between fixed and mobile devices over short distances with 2.4 GHz radio. Moreover, the chip of Bluetooth 4.0 consumed less energy than normal Bluetooth, and it was often used on healthcare, fitness or beacons. Although Bluetooth 4.0 was developed with ultra-low power consumption (150-250 uW) and longer communication range, it couldn't run with a single battery for a lifetime. Therefore, it was important to use energy harvesting techniques to extend its battery life. Additionally, there were several GAP roles, Generic Access Profile, in Bluetooth to determine how two devices could communicate with each other. [11] The two main roles were peripheral and central. The peripheral role could send small chunks of data in a low power mode, and it could work as an advertiser. However, it couldn't modify the connection parameter itself when connecting to the central device but could terminate the connection device intentionally. The central role worked as a scanner. It would send out a request to the peripheral device for sending the data packet. If the peripheral device accepted the request from the central device, a connection would be established. We could see the relation between the two roles in Figure 4.

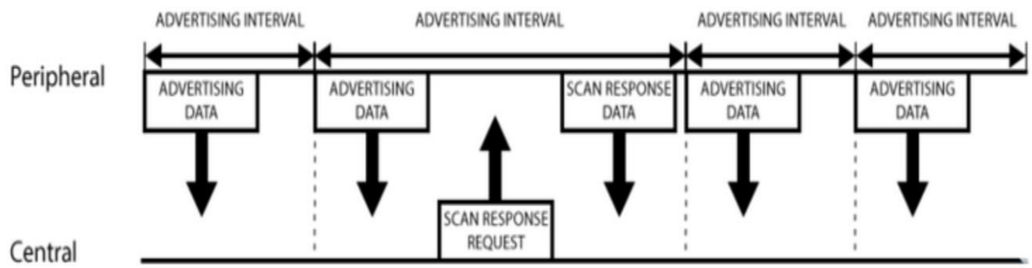

Figure 4. GAP roles of peripheral and central. [17]

In addition to understanding the basic mode, we also need to know the limitation of the sample rate. The original testing sample rate was 1000 Hz. Nevertheless, according to the online journal "Electrocardiogram Sampling Frequency Range Acceptable for Heart Rate Variability Analysis", it said that 500 or 250 Hz resulted in excellent concordance with 1000 Hz. [12] Therefore, our goal was to make the sensor be able to read at least 250 data per second and send out the data to the mobile application.

1.2 Principle

1.2.1 Instrument amplifier

An instrumentation amplifier was a type of differential amplifier and had a precision gain. It amplified the difference between two input signal voltages into one signal. Therefore, the amplifier was often used on measurement and test equipment.

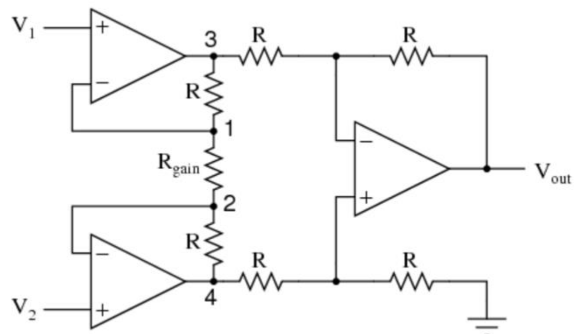

Figure 5. Instrument amplifier. [12]

1.2.2 High pass filter

High pass filter (HPF) was an electronic filter that only allowed the frequency of signals which was higher than the selected cut-off point, and reduced any low-frequency signals.

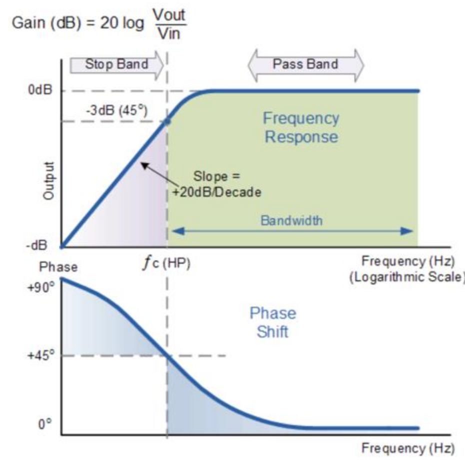

Figure 6. 1st Order High Pass Filter. [13]

1.2.3 Lowpass filter

Low pass filter (LPF) was an electronic filter that only allowed the frequency of signals which was lower than the selected cut-off point, and reduced any high-frequency signals.

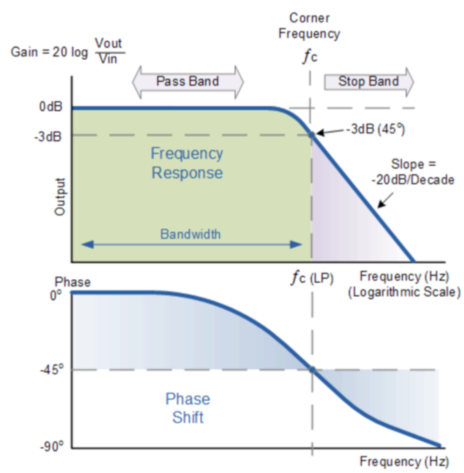

Figure 7. 1st Order Low Pass Filter. [14]

1.2.4 Operational amplifier

An Operational Amplifier (op-amp) was fundamentally a voltage amplifying device designed to be used with external feedback components. It had three terminal which consisted of two high impedance input. The value of the gain would depend on using inverting input, a non-inverting input, and the resistors.

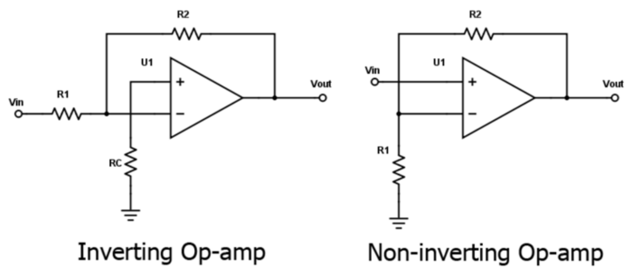

Figure 8. Operational amplifier. [15]

1.2.5 Notch filter

A notch filter was a kind of band-stop filters which could narrow stopband in order to remove a particular frequency.

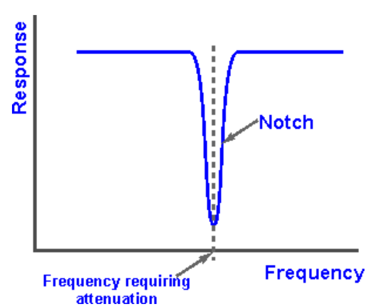

Figure 9. Notch Filter. [16]

1.3 Introduction

According to the awakening of wellness consciousness, people seek to find a piece of equipment that could monitor their health condition in a stable and long-term way. Although there are many health monitor systems on the market nowadays, they are not easy to carry around. In addition, the sensor is unable to be long-term and continuous monitoring; the traditional circuit system is a rigid structure that does not meet the requirements of the new flexible measurement; the measurement system has a single function and cannot simultaneously perform multiple physiological monitoring of the same person's physical condition. In response to this problem, our study proposes to provide several options for making the monitor more wearable and functional. Flexible electronic brings innovations to the electronic technology field. It is the newest and the most potential of large-area electronics. Nowadays, electronics are mostly made of silicon wafers, which are stiff and not elastic. However, the recent advance in silicon-based polymers film provides new routes to build circuits, which offers the searchability of electrical properties. Rigid electrical components standing on flexible substrates (mostly silicon-based polymers) with the serpentine or wavy connection is the most widely used structure for flexible electronics. Therefore, after reading lots of literature, we plan to design a device circuit includes multiple sensors, energy harvesting system in order to detect different health data and have longer lifetime device. This circuit design can be assembled like children building blocks, switching different sensors to measure different data, such as ECG, EMG, temperature or PH value. Besides, we will need the knowledge of flexible electronics in order to understand the limitation of flexible electronics for our design. We will also include a wireless communication antenna to provide the device with a solution for wireless data transmission. We believed that the wireless modulus could bring many advantages such as less motion influence, longer distance monitor, and more flexible to be carried. We will need to write our own wireless program in Nordic system environment. We expect to have a device that is able to read ECG signal and human skin temperature and send to mobile application at the end of research.

Chapter 2 -Methodology

2.1 Design plan & equipment used

2.1.1 Customer needs

Before we start our project, we want to determine what our priority for our research is. We know that there are many commercial and medical health monitors in the market. Their prices are from hundred to thousand dollars, which is not affordable for a normal family. Besides, we consider that our system is used for health monitoring, so it should need to work in the long term. Therefore, we would need to pay attention to the power consumption of the device. The following Table 1 is the list of customer needs and its priority-ranked that I discussed with Jia Zhu.

Table 1: A priority-ranked list of customer needs.

Customer needs	Ranked (1-less important – 3- most important)
Retail cost	1
Form factor: size, weight, described qualitatively	3
Durability	2
Lifespan in years/ service repair	1
Usage environment	2

Lower power consumption	3
Two sensors required	3

2.1.2 Engineering requirement

In this section, we want to translate the features and performance requirements described in the customer needs to engineering specifications. We want to put our budget for major components, such as amplifiers, bluetooth, resistors, and capacitors. In addition, we are concerned about the device which would be carried around, so the size of the device should be easy to carry or be kept inside the pocket. Besides, the power dissipation of the device should be as low as possible in order to extend battery life.

Table 2: A "Translated" list of engineering requirement.

Customer needs	Engineering requirements
Retail cost	• Cost of finished good • Budget for major components
Form factor: size, weight, described qualitatively	Size of the system should not over 40mm x 60 mm x 15mm.
Durability	• Bending strength • Stretch strength • Impact strength (drop test criteria)
Lifespan in years/ service repair	Cycles of critical components / Enable to repair
Usage environment	Operating temperature range (room temperature)
Lower power consumption	Total power consumption: 40 mW
Two sensors required	• Temperature sensor (thermistor) • Electrophysiological sensor

2.2 Methods

The aim of this research is to design a multi-function wireless monitoring system. For instance, the design, resembling a monitor system for human physiological conditions, is also flexible and extensible. Our solution provides a microcontroller with two different sensors (temperature and electrophysiological) in order to implement multi-sensing simultaneously. We also reserve spaces for other sensors that we will add in the future. In our design, we selected wireless charge batteries for the power supply of our whole embedded system since NFC power source was not stable and only had 1.5 V. Furthermore, we built our own electrophysiological sensor (ECG sensor), consisting of an instrumental amplifier, high pass filter, low pass filter, non-inverting amplifier, and notch filter. We chose AD623 as our instrumental amplifier because it was a single and dual-supply amplifier, with low power consumption. If we wanted to change our power supply to the NFC system, which would only supply single voltage in the future, we would need to use an amplifier that allowed us to do so. After designing the power system, we set the cut-off frequency of high pass filter at 0.5 Hz, and the cut-off frequency of low pass filter at 150 Hz to reduce noise and get a better ratio of S/N (Signal to noise). Moreover, we used a non-inverting amplifier with 5 gains to increase the output signal and added a notch filter to reduce the noise to 60 Hz, which is the standard frequency requirement for buildings in the U.S. After assembling the ECG sensor, we focused on the temperature sensor by using lm19, a CMOS integrated-circuit temperature sensor. Lastly, we set up our Bluetooth modulus (nrf51822) and connected it to the output of both sensors to serve the flow of messages through the mobile application.

Chapter 3 -Testing Progress & Results

In the beginning of the research, we wanted NFC to be both the power source and the wireless communication channel. However, the measured output voltage, which was around 1.5 V, was too low and not stable enough to be our power source. Although we used a 5V power source to test the circuit in the lab, we decided to use a wireless charge battery ranging 3.3V in the actual device. We understood that the ECG signal was low in amplitude (1µV~1mV) and noisy. Also, the skin impedance was between 10kΩ and 200kΩ [8]. As a result, we needed amplifiers to increase the output and multiple filters to control the frequency range in order to minimize the noise. In our experiment, we used Multisim, a circuit design software, to simulate our circuit design. We have an instrument amplifier (AD623) to combine two signal inputs into one signal output. The input signal is applied to PNP transistors, acting as voltage buffers and providing a common-mode signal to the input amplifiers. An absolute value 50 kΩ resistors in each amplifier feedback assures gain programmability. Hence, we can use the following equation to calculate the differential output.

$$V_o = (1 + \frac{100\ k\Omega}{R})V_i$$

In this case, we chose a 5.1 kΩ resistor, but the real value of the resistor was 5.02 kΩ, so the output gain would be 20.9. Next, we had a passive second order high pass filter and an active second order low pass filter to control the frequency range between 0.5 Hz and 150 Hz. We chose to use a second order filter because the reaction of the filter is much faster, and it improved our sensor resolution. Then, we had another non-inverting amplifier with 5 gain to increase our voltage output again. Lastly, we used a notch filter with a cutoff frequency at 60 Hz to reduce the impact of the noise. The simulation can be seen in Figure 10&11. We also simulated the power dissipation of the system, which was 3.778 mW for the ECG sensor.

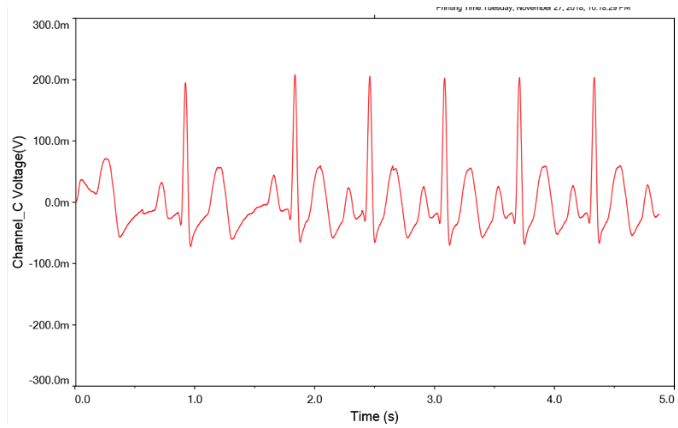

Figure 10. ECG sensor output simulation.

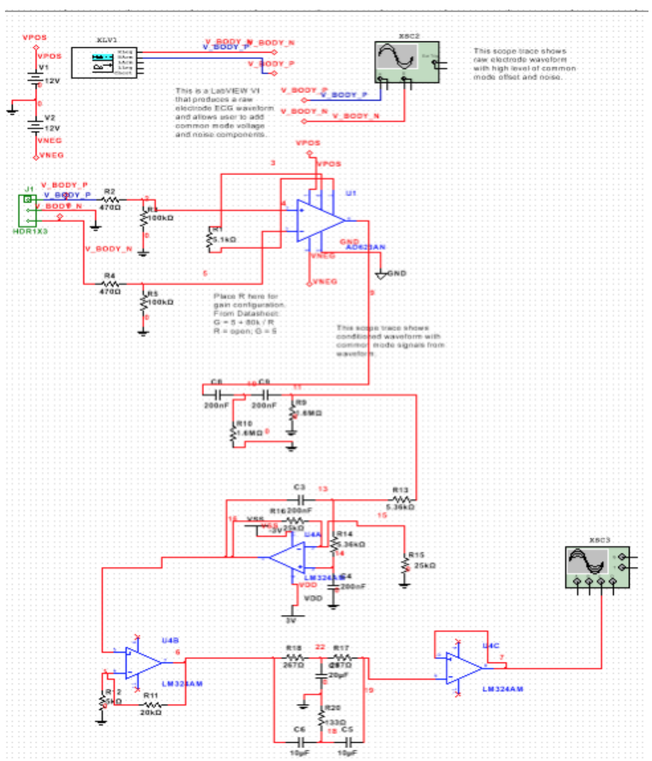

Figure 11. Circuit of the ECG sensor simulation.

We could see our circuit design of ECG sensor work properly, so we started assembling the hardware circuit, which is shown in Figure 12. The circuit consisted of an ECG sensor, a temperature sensor, and a Bluetooth microcontroller.

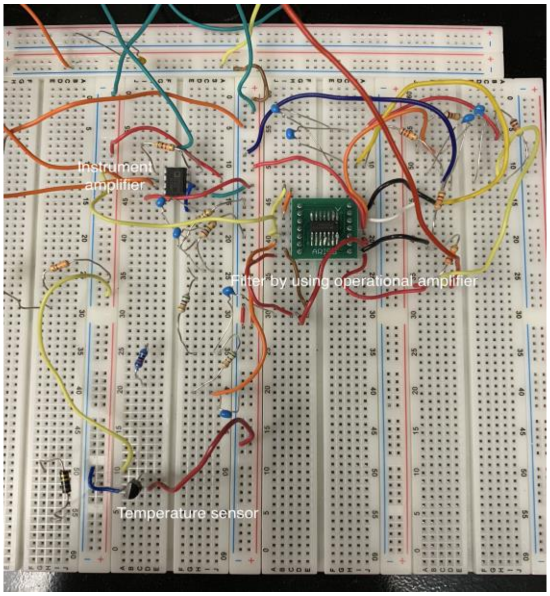

Figure 12. The circuit of ECG sensor.

To verify the function of each of the filters in ECG sensor, we used the bode analyzer in myDAQ tool. The resolution can only support frequency from 1 Hz to 10 kHz, therefore, the bode value from the device is not accurate. The diagram, however, can show whether our circuit has issues. We, then measured the real resistor values of high pass filter and low pass filter. The value was 1.64MΩ, 1.61MΩ, 5.5kΩ, and 5.51kΩ respectively. Hence, we can use the formula of the second order cut-off frequency to determine the percentage error between the result and theoretical value. The capacitors we used for both filters were 220 nF.

$$\text{Cut-off frequency:} \quad f_c = \frac{1}{2\pi\sqrt{C_1 C_2 R_1 R_2}}$$

Consequently, we found out that the cut-off frequency of the high-pass filter was 0.445 Hz, and the cut-off frequency of the low-pass filter was 131.41 Hz in theory. In the following Figure 13 & 14, the value we got from the bode analyzer was 1.17 Hz and 158.49 Hz. The percentage of error was 61% and 17% respectively. The error was quite big because these values from bode analyzer were not exact at 3dB.

However, the analyzer indicated that our filter was working properly to cut off a certain frequency. We would adjust the resistors' value, if necessary in the later experiments.

Theoretical high-pass cut-off frequency: $f_c = \frac{1}{2\pi\sqrt{220*220*10^{-9}*10^{-9}*1.64*1.61*10^{6}*10^{6}}} = 0.445\ Hz$

Theoretical low-pass cut-off frequency: $f_c = \frac{1}{2\pi\sqrt{220*220*10^{-9}*10^{-9}*5.5*5.51*10^{3}*10^{3}}} = 131.41\ Hz$

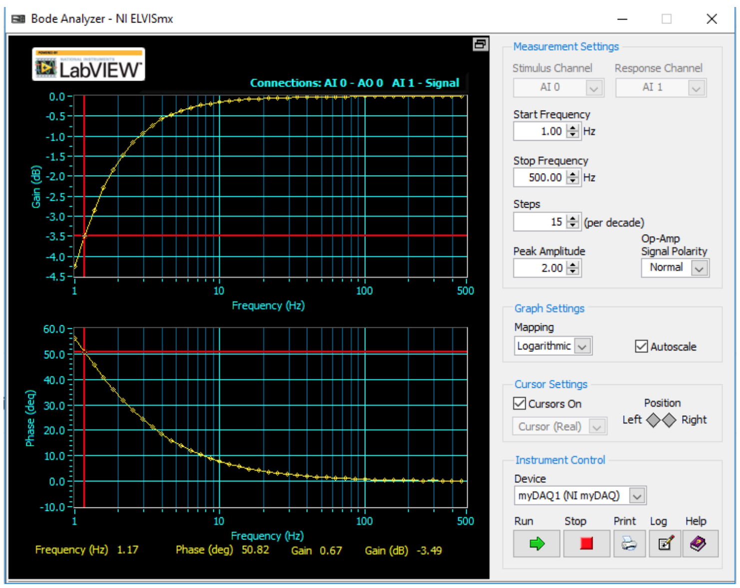

Figure 13. High-pass filter bode diagram.

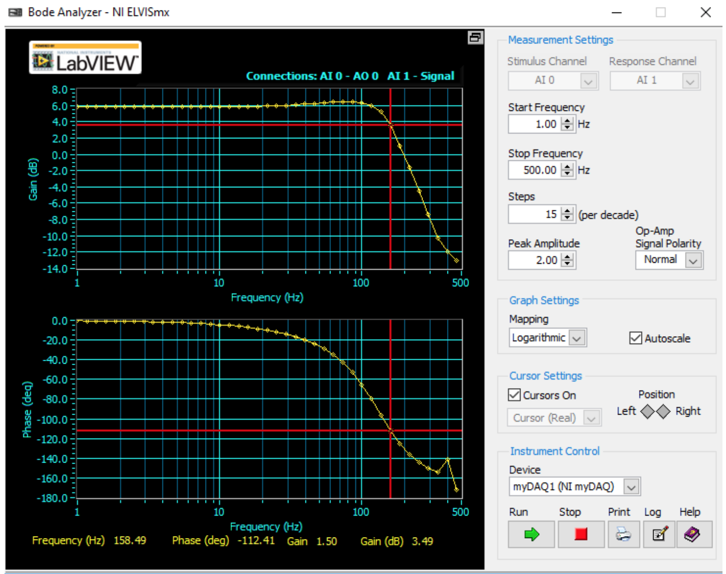

Figure 14. Low-pass filter bode diagram.

We did the same progress on the notch filter. The resistor value was 11.9 kΩ, 11.77 kΩ, and 6.15 kΩ. The capacitor value was 220 nF of each. We used two capacitors in parallel to get the value 440 nF since we cannot find the capacitor in that value. The result that we got from the calculation was 58.8 Hz, and the number from the bode diagram was 54.12 Hz. Hence, the percentage of error was 7.98%. Moreover, we had noticed that the gain was slightly increased after the cut-off frequency. In our opinion, the increased signal was occurred when myDAQ reboot the testing signals through our device.

Figure 15. Notch filter bode diagram.

Although the percentage of error didn’t meet our expectation, the bode diagram was matched to the theoretical diagram. Consequently, we set up our ECG sensor and a bio-amplifier, which was a medical used sensor, to monitor our ECG signal simultaneously. Both ECG sensors were connected to an acquisition system, Powerlab, and sent the data to the computer software. The overall result is displayed in Figure 17. To analyze the data carefully, we replot the diagram by using Origin pro data analysis software. We made the plot in a certain time slot, so we could observe the signal peak of the data precisely.

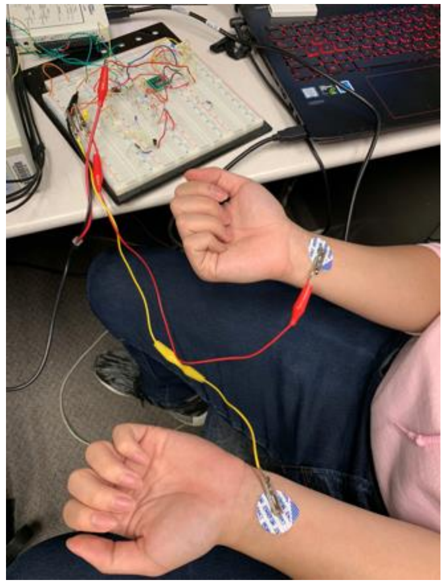

Figure 16. ECG testing.

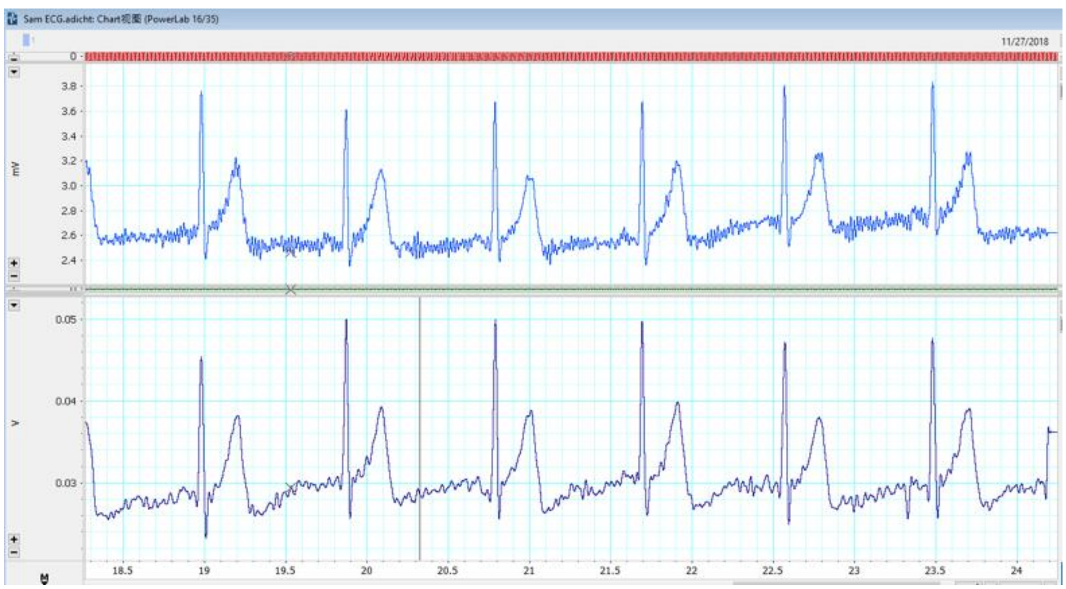

Figure 17. ECG diagram from bio amplifier sensor (top) and our own ECG sensor (bottom).

Figure 18 is the overall data of our own ECG sensor, and Figure 20 is the data from the bio-amplifier. We, then zoomed both plots in the time scale between 33 seconds and 37 seconds to see the signal wave carefully.

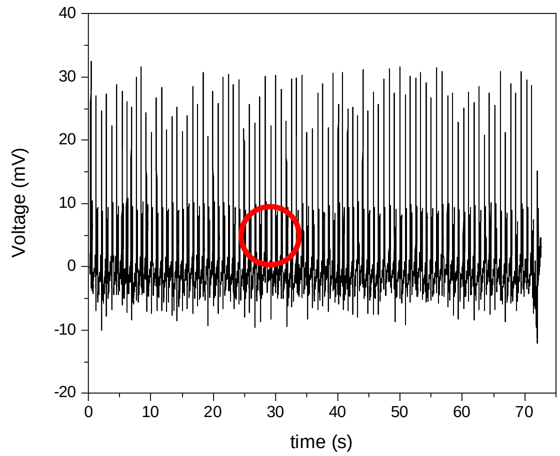

Figure 18. Own design ECG diagram.

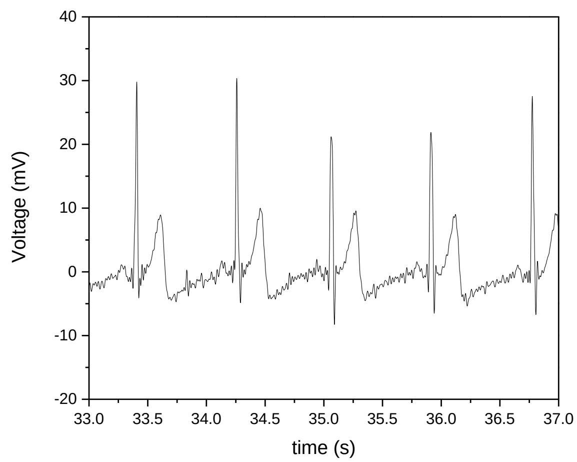

Figure 19. Data zoom in at the red circle.

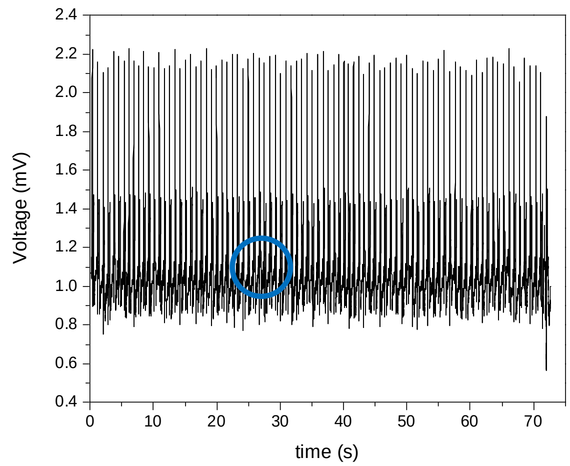

Figure 20. Bio amplifier ECG diagram.

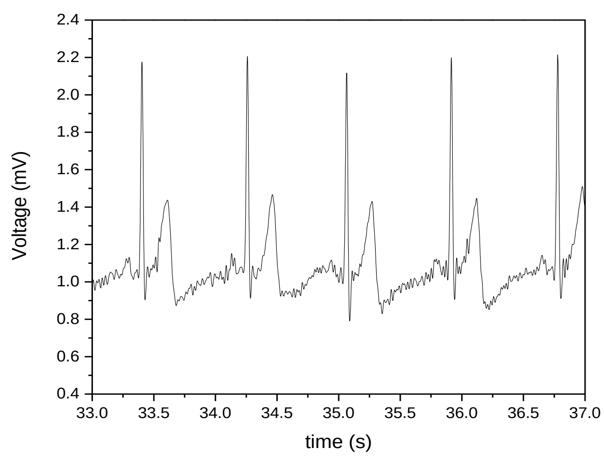

Figure 21. Data zoom in at the blue circle.

From the diagram, we can see both waves have the same pattern, but the voltage is ten times different, which we can see easier in Figure 22. The reason why their voltages are different is that the gain of bio amplifier is 10, and the gain of our sensor is 103.3, which is calculated by the gain of instrument amplifier 20.9 V/V times the gain of the non-inverting amplifier 4.94 V/V. To compare the difference between both ECG diagrams, we decided to overlap both diagrams together by timing 10.3 of the data of the bio amplifier. Also, we noticed that there is an 1 mV offset in the diagram of bio amplifier, so we subtracted 10.3 V in the end. We will discuss later why there is an offset occurred in bio-amplifier. Hence, we can compare both waves easily in Figure 23 & 24. Both waves can obviously determine PQRST points, which are important parameters for ECG signal, but the trend of the wave of our sensor is more obvious. Nevertheless, the signal of our sensor was not flat at a red dot, which we will discuss later as well.

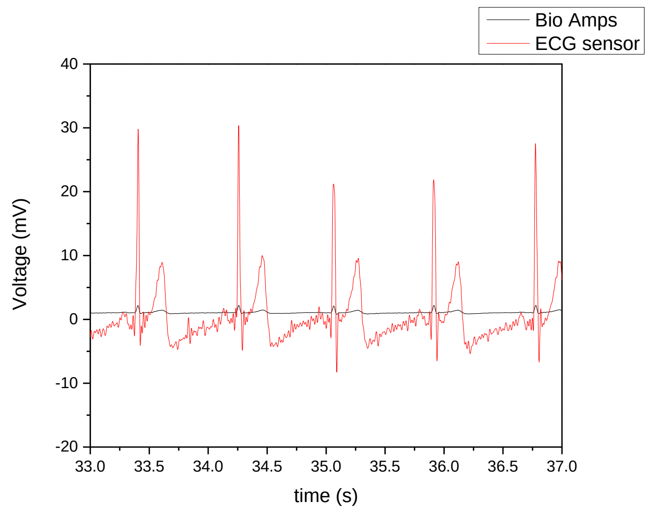

Figure 22. Comparison of both ECG diagram in origin scale.

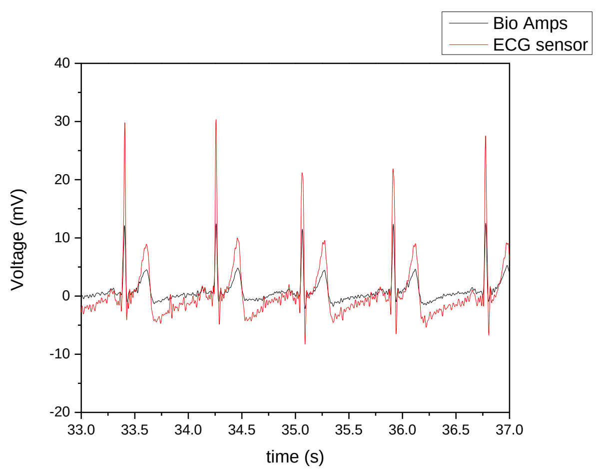

Figure 23. Comparison of both ECG diagram in adjustment scale of 10.3.

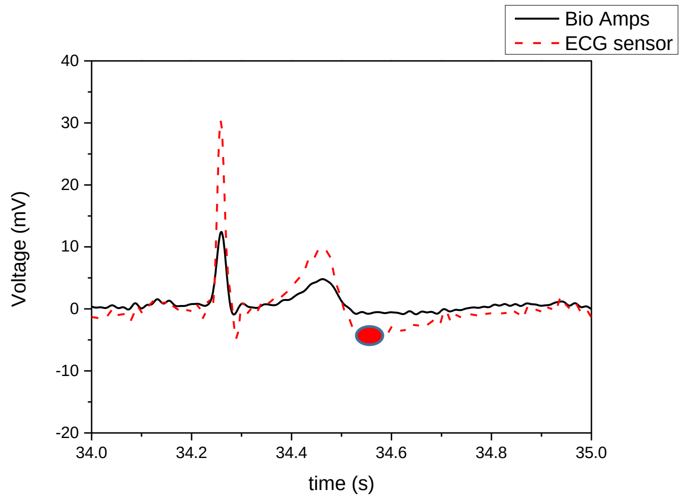

Figure 24. Comparison of both ECG waves in a second.

We can determine that our design of an ECG sensor was successful since we can see the diagram of our sensor had a pretty similar pattern as the diagram of the bio-amplifier. After finishing the assembly of ECG sensor, we chose a CMOS integrated-circuit (lm19) to be our temperature sensor because it can monitor a wide range (−55°C to +130°C) with high precision. Then, we needed to make the microcontroller inside the Bluetooth chips (nrf51822), which shows in Figure 25, be able to read the analog output from both sensors and send the digital data back to the mobile application. The code is shown in Appendix A.

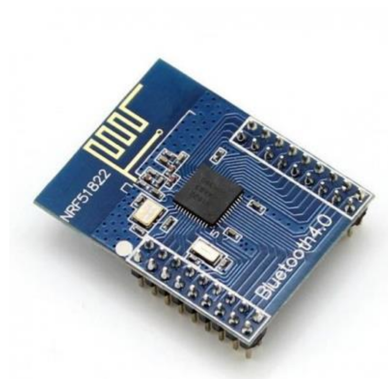

Figure 25. Bluetooth chip (nrf51822).

In our initial calibration, we got the values 2.02 V and 3.02 V respectively. However, in order to get the desired voltage 2 V and 3V, we had calibrated the ADC reader in Bluetooth by subtracting 0.02 V. We used it to test both temperature and ECG sensors. It worked properly to show the ADC value of both sensors.

We, then have to compare the previous results with the data we received from Bluetooth in Figure 26. We plotted an ECG graph by using the data we collected from Bluetooth, and we realized that the data points are disordered. We believed that our phone did not receive enough data because of the receiving limitation of the mobile application. We will explain the results in the discussion later.

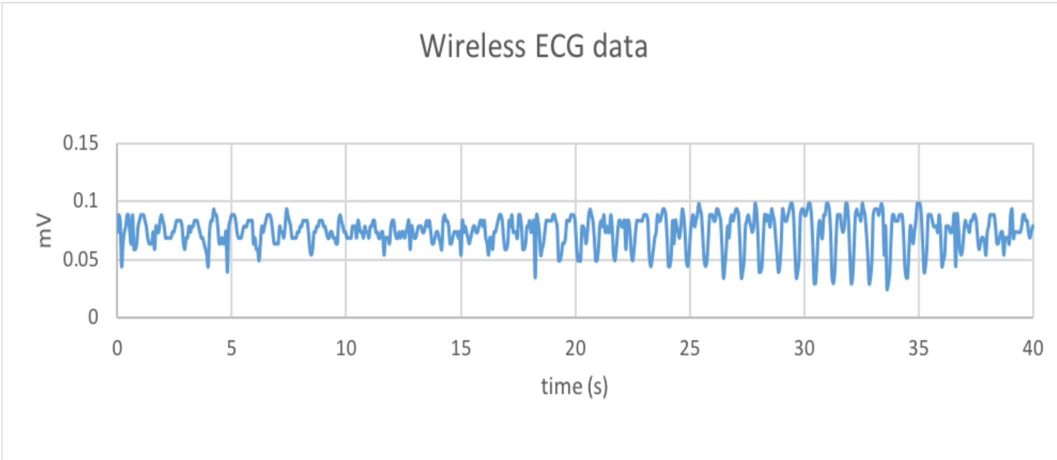

Figure 26. ECG signal data from mobile application.

Because we need to have better receiving speed rate of the mobile application, we will need to create our own Bluetooth wireless application in the future. Although we cannot draw the ECG diagram properly, the ADC value we received is accurate. We used the oscilloscope to verify the temperature sensor voltage value which we received from Bluetooth. We will need to convert the ADC value to voltage, using the equation which showed in below to calculate the value. The ADC reports a ratio metric value, and our voltage input is 3.6 V for the system. This means that the ADC assumes 3.6V is 1023 and anything less than 3.6V will be a ratio between 3.6V and 1023. In the following table 3, there is the value of oscilloscope and Bluetooth.

$$\frac{Resolution\ of\ the\ ADC}{System\ Voltage} = \frac{ADC\ Reading}{Analog\ Voltage\ Measured} = \frac{1023}{3.6\ V}$$

Table 3. Voltage measurement from Bluetooth and Oscilloscope.

ADC	Blue-Voltage (V)	Osc-Voltage (V)	%Difference
459	1.615249267	1.588	1.715948795
460	1.618768328	1.59	1.809328833
455	1.601173021	1.569	2.050543055
452	1.590615836	1.565	1.636794618
450	1.583577713	1.558	1.641701708
448	1.576539589	1.551	1.646653091
447	1.573020528	1.549	1.550711934
446	1.569501466	1.544	1.65164937

From the table, we can see that the voltage which was detected by Bluetooth is slightly larger than the data from the oscilloscope. The percentage difference can also see in the table, which is smaller than 5 %, which means that our Bluetooth communication is reliable. By calculating the voltage, we could transfer these values into a temperature number in Celsius. The equation is provided on the datasheet of the temperature sensor, which is shown in below.

$$T = -1481.96 + \sqrt{2.1962 \times 10^{6} + \frac{(1.8639 - V_O)}{3.88 \times 10^{-6}}}$$

The equation provided us a relationship between voltages and temperature and we added this equation in our wireless program, so we can see the temperature value directly from the mobile application, which is shown in Figure 27.

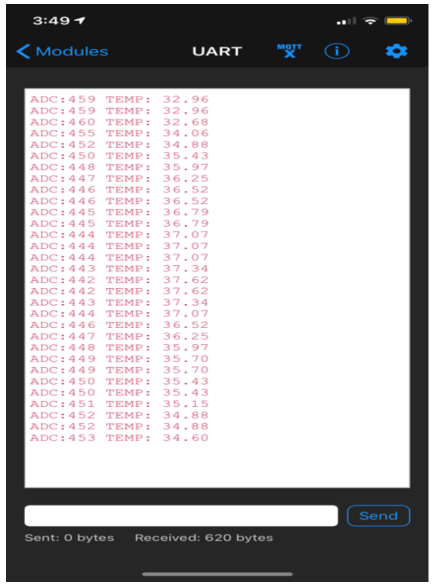

Figure 27. Bluetooth screen.

In the end, we had successfully made a multiple sensor monitor with a wireless communication function. However, there are still many parts that should be improved. We will like to add more sensor on our device such as EMG, EEG or PH value. Electromyograms, EMG signal is useful for assessing the health of the neuromuscular system. EEG is an electrophysiological method to record the electrical activity of the brain. pH value in the chemical is a scale used to specify how acidic or basic a water-based solution is, and it is important for humans' bone health. This data does not require high sample rate, so we believe they will work properly. We will test them later on. Our final goal is to create a wireless small health monitor, which can not only be easily carried around but also have a higher resolution for medical use. Also, we hope this device can be assembled like the child building blocks. For example, when we want to detect ECG signal, we can add the ECG sensor on the device. When we want to measure PH value, we just need to replace the ECG sensor to PH sensor of the device. The block diagram is showed in Figure 28.

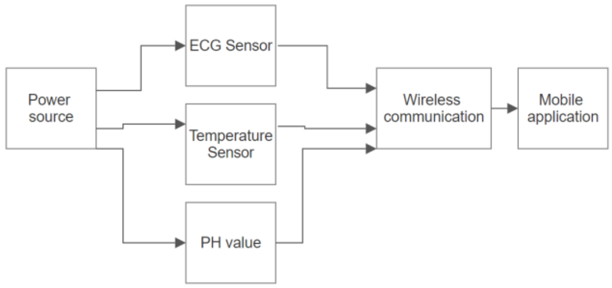

Figure 28. Block diagram of the device.

Moreover, we understand how important wireless communication of the device is, which can reduce the use of large measurement instruments and interference. The technique can be implemented in many different areas. In the later section, we will discuss our results and find solutions to improve our research.

Chapter 4 -Discussion

According to the diagram of the result, we can see the voltage scale is different. The reason is that the gain of our design is 100, and the gain of the bio-sensor is 10. Besides, we notice that there is a DC offset in Figure 21, the data from bio-amplifier. Normally, the actual desired signal is ±0.5mV superimposed on the electrode offset. In addition, the system also picks up the 50/60Hz noise from the power lines which forms the common mode signal, which needs to be filtered. [19] We can tell the difference from the data which monitor by our design sensor because we assemble a notch filter in our sensor which could reduce the 50~60 Hz noise. However, when we put both data points together in Figure 24, we notice that there is a negative offset at red point. We think that a high pass filter causes undershoot after the QRS complex. [19] In order to eliminate the drift, we may need a simple resistor divider to be a DC common-mode feedback. As I interviewed my friend, Lin, who is a medical student in National Taiwan University, he told me that the important thing about the ECG signal was the parameters of PQRST points. The doctor can tell the patients' condition by observing P wave, QRS complex, and ST segment. For example, the ST segment can determine the diagnosis of ventricular ischemia or hypoxia. Hence, it is important to present the signal wave precisely, and our ECG sensor can successfully show these points and have a slightly difference with the result of the bio-amplifier. Although we cannot plot the ECG diagram by using wireless application, we still get a good wave shape from the analyzer. We studied and found out that there is a speed limit of BLE and hardware limit of the Bluetooth chip. We used nrf51822 with S110 softdevice for our Bluetooth programming environment. When the softdevice is enabled, the CPU will be blocked for approximately 0.8 to 6 ms. The time will be determined by how many packets we send per time. If sending one packet per connection event, then the CPU is blocked for about 1 millisecond which limits the ADC sampling frequency to around 1 kHz. If six packets per connection event are sent, then the CPU is blocked for about 6 milliseconds which will limit the ADC sampling frequency to around 150 Hz.

[20] But, there is a speed limitation for mobile application as well. Different types of operating system will have different speed to send out packets per connection interval. We can see the numbers in Figure 29.

- **iPhone 5/6 + IOS 8.0/8.1**
  6 packets * 20 bytes * 1/0.030 s = 4 kB/s = 32 kbps
- **iPhone 5/6 + IOS 8.2/8.3**
  3 packets * 20 bytes * 1/0.030 s = 2 kB/s = 16 kbps
- **iPhone 5/6 + IOS 8.x with nRF8001**
  1 packet * 20 bytes * 1/0.030 s = 0.67 kB/s = 5.3 kbps
- **Nexus 4**
  4 packets * 20 bytes * 1/0.0075 s = 10.6 kB/s = 84 kbps
- **Nordic Master Emulator Firmware (MEFW) with nRF51822 0.9.0**
  1 packet * 20 bytes * 1/0.0075 = 2.67 kB/s = 21.33 kbps
- **Nordic Master Emulator Firmware (MEFW) with nRF51822 0.11.0**
  6 packets * 20 bytes * 1/0.0075 = 16 kB/s = 128 kbps

Figure 29. Speed limit for different operating system. [21]

Therefore, we will need to develop our own mobile application by using open sources on the internet or LabVIEW environment in the future. All in all, our goal of this research is provided us a method to deal with multiple health/physical condition. When we look at the data of temperature we received from our mobile application, we notice that our circuit of the wireless channel can communicate successfully. The programming we wrote make the Bluetooth chip be able to read the voltage output from either ECG sensor or temperature sensor simultaneously. Although making wireless communication is not a new technique, our design provides a low power consumption mode (approximately 5 mW by simulation), which is able to wear the device in a long-term situation. Moreover, we get inspiration from this research and find out how important wireless monitor technology is. The graduate student, Ning Yi, in our lab has developed a water-soluble electrode, which can perfectly contact on human skin. Hence, we will combine both of our research together since the design of soluble electrode can help us get more accurate data and also reduce the interference of the wires and movements.

Chapter 5 -Conclusion

In this paper, we observed that the results between the bio-amplifier sensor (medical use) and our ECG sensor are pretty similar. Therefore, we can conclude that our ECG sensor is successful. Besides, our Bluetooth modulus can successfully send ADC values of both sensors, which allows us to use it as wireless monitoring for other experiments. The next step is to improve the power source of the embedded system for better stability and add more sensors to the device. In our future work, we will also aim to design a new mobile application which features the ECG plot drawn for the Bluetooth module.

In conclusion, we have presented a solution to the previously expensive hardware health monitor. The components used in our solution cost $11 in total, which is only a tiny fraction compared to the cost of state-of-the-art health monitor and thus is extremely affordable for the community. We also contribute to improving the ECG signal quality by controlling the filter and providing better electrode-to-patient contact. In addition, the device can simultaneously send multiple data packets to the mobile application. Therefore, the impact and benefits of our multi-sensing system to both the community and the research space will be groundbreaking in the future. We believe that enhancement on making sensors more flexible to wear and hence improving the stability in the long-term for physiological condition monitoring is a crucial direction for further research.

Appendix A

Keil code for Bluetooth

```
int main(void)
{
    uint32_t err_code;
    bool erase_bonds;
    uint8_t  start_string[] = START_STRING;


    // Initialize.
    APP_TIMER_INIT(APP_TIMER_PRESCALER, APP_TIMER_OP_QUEUE_SIZE, false);
    uart_init();
    buttons_leds_init(&erase_bonds);
    ble_stack_init();
    gap_params_init();
    services_init();
    advertising_init();


    conn_params_init();
    printf("%s",start_string);
                        printf("\n\rADC HAL simple example\r\n");
    printf("Current sample value:\r\n");
    err_code = ble_advertising_start(BLE_ADV_MODE_FAST);
    APP_ERROR_CHECK(err_code);
        // Enter main loop.
```

```
while(true)
{
        adc_1();
        adc_2();
    // trigger next ADC conversion
    //nrf_adc_start();
  // enter into sleep mode
  __SEV();
  __WFE();
  __WFE();
        uint8_t str[4];
        sprintf((char*)str, "ADC:%d TEMP: %.2f",
(int)adc_result,(float)tempvalue);// out ADC result
        ble_nus_string_send(&m_nus, str, strlen((char*)str));
    nrf_delay_ms(2000);
        sprintf((char*)str, "ECG-ADC: %d", (int)adc_output);
        ble_nus_string_send(&m_nus, str, strlen((char*)str));
    nrf_delay_ms(2000);
        power_manage();
}
}
/**
 * @}
 */
```

Appendix B

Components list

Instrument amplifier:

- AD623A*1

Operational amplifier:

- LM324*1

Resistor:

- 330 Ω*1
- 5.1 KΩ*2
- 5.6 KΩ*2
- 6 KΩ*1
- 12 KΩ*2
- 20 KΩ*1
- 1.6 MΩ *2

Capacitor:

- 220 nF*7

Thermistor:

- Lm19 *1

Blue modulus:

- NRF51822

BIBLIOGRAPHY

1. Huang, Z., Hao, Y., Li, Y., Hu, H., Wang, C., Nomoto, A., ... & Li, W. (2018). Three-dimensional integrated stretchable electronics. Nature Electronics, 1(8), 473. 2.Maximintegrated. (2012, March 29). Energy Harvesting Systems Power the Powerless. Retrieved from https://www.maximintegrated.com/en/app-notes/index.mvp/id/5259
2. Brunelli, D., Moser, C., Thiele, L., & Benini, L. (2009). Design of a Solar-Harvesting Circuit for Batteryless Embedded Systems. IEEE Transactions on Circuits and Systems I: Regular Papers, 56(11), 2519-2528. doi:10.1109/tcsi.2009.2015690
3. Bibo, A., Masana, R., King, A., Li, G., & Daqaq, M. F. (2012). Electromagnetic ferrofluid-based energy harvester. Physics Letters A, 376(32), 2163-2166.
4. Wahbah, M., Alhawari, M., Mohammad, B., Saleh, H. H., & Ismail, M. (2014). Characterization of Human Body-Based Thermal and Vibration Energy Harvesting for Wearable Devices. IEEE J. Emerg. Sel. Topics Circuits Syst., 4(3), 354-363.
5. Siddique, A. R. M., Rabari, R., Mahmud, S., & Van Heyst, B. (2016). Thermal energy harvesting from the human body using flexible thermoelectric generator (FTEG) fabricated by a dispenser printing technique. Energy, 115, 1081-1091.
6. Hughes, M. (2018, August 03). Wireless RF Energy Harvesting: RF-to-DC Conversion and a Look at Powercast Hardware. Retrieved from https://www.allaboutcircuits.com/technical-articles/wireless-rf-energy-harvesting-rf-to-dc-conv ersion-powercast-hardware/
7. Clark, S. (2011, November 08). NFC goes green: New ST chips use energy harvesting to replace the need for batteries • NFC World. Retrieved from https://www.nfcworld.com/2011/11/08/311126/nfc-goes-green-new-st-chips-use-energy-harv esting-to-replace-the-need-for-batteries/

8. Chen, H.S., Huang, Z.X. (December 29, 2004). The Circuit Design and Implementation of Ambulatory Multiple – lead ECG. Retrieved from http://www.auto.fcu.edu.tw/wSite/public/Attachment/f1255510681794.pdf
9. Lacirignola, F., & Pasero, E. (2017, September). Hardware design of a wearable ECG-sensor: Strategies implementation for improving CMRR and reducing noise. In Circuit Theory and Design (ECCTD), 2017 European Conference on (pp. 1-4). IEEE.
10. Willem Einthoven. (2016, March 8). Retrieved from https://ethw.org/Willem_Einthoven
11. Huang, Z., Hao, Y., Li, Y., Hu, H., Wang, C., Nomoto, A., ... & Li, W. (2018). Three-dimensional integrated stretchable electronics. Nature Electronics, 1(8), 473.
12. Allaboutcircuits. (n.d.). The Instrumentation Amplifier. Retrieved November 28, 2018, from https://www.allaboutcircuits.com/textbook/semiconductors/chpt-8/the-instrumentation-amplifi er/
13. Electronicstutorials. (2018, May 15). High Pass Filter - Passive RC Filter Tutorial. Retrieved from https://www.electronics-tutorials.ws/filter/filter_3.html
14. Electronicstutorials. (2018, May 15). Low Pass Filter - Passive RC Filter Tutorial. Retrieved from https://www.electronics-tutorials.ws/filter/filter_2.html
15. Allaboutcircuits. (n.d.). Non-Inverting Op-Amp Resistor Calculator. Retrieved November 28, 2018, from https://www.allaboutcircuits.com/tools/non-inverting-op-amp-resistor-calculator/
16. Poole, I. (n.d.). Op Amp Notch Filter Circuit. Retrieved from https://www.radio-electronics.com/info/circuits/opamp_notch_filter/opamp_notch_filter.php
17. Shrestha. B. (October 6, 2016). Measurement of power consumption of BLE (Bluetooth Low Energy). Retrieved March 21, 2019, from https://www.theseus.fi/bitstream/handle/10024/118662/Shrestha_Bikash.pdf?sequence=1&isAllowed=y

18. Kwon, O., Jeong, J., & Kim, H. B. (2018, July). Electrocardiogram Sampling Frequency Range Acceptable for Heart Rate Variability Analysis. Retrieved from https://www.ncbi.nlm.nih.gov/pmc/articles/PMC6085204/

19. Bharadwaj, A., Kamath, U., & Cypress Semiconductor Corp. (2011, February 14). Techniques for accurate ECG signal processing. Retrieved from https://www.eetimes.com/document.asp?doc_id=1278571

20. Sverrisson, S. B. (2014, November 28). Using the ADC with the S110 SoftDevice. Retrieved from https://devzone.nordicsemi.com/b/blog/posts/using-the-adc-with-the-s110-softdevice

21. Townsend, K. (2018, December 14). Introducing the Adafruit Bluefruit LE Friend. Retrieved from https://learn.adafruit.com/introducing-adafruit-ble-bluetooth-low-energy-friend/faq

ACADEMIC VITA

Junghsien Wei

211 Levashire Heights Apt 304 State College, PA, 16803

jung.hsien.wei@gmail.com

Education

2015-2019 Bachelor of Science in Electrical Engineering and Engineering Science

The Pennsylvania State University, University Park, PA

Penn State University Schreyer Honors Scholar

2012-2015 Graduated with Distinguished Academic Record Award Diploma Kaohsiung Municipal of Kaohsiung *Senior High School, Kaohsiung, Taiwan*

Honors and Awards

2016 – President's freshman Award

2015 – Certificate of Achievement in engineering design competition

Association Memberships/Activities

Member, Engineering Undergraduate Council in the College of Engineering 2015 Member, Penn State sailing club 2015

Member, Penn State boxing club 2015

Member, National Society of Collegiate Scholars 2015-present

Member, Tau Beta Pi the engineering honor society 2017-present

Professional Experience

Undergraduate Research Assistant

Title: Improvement of serpentine networks for crack resistance

• Studied the influence of breaking lines in networks on the mechanical stiffness of composite substrates.

• Created own motion stage and load cell monitor by Arduino.

Title: The design of a multi-sensing flexible system used for real- time monitoring.

• Converted a traditional electronics system into flexible and wearable application.

• Created NFC (Near-field communication) as a power supply for the circuit.

• Managed Bluetooth modulus to send out signals of electrophysiology and temperature.

Lab Assistant in SolidWorks

Department of Engineering Design in the College of Engineering, University Park, PA

• Managed student design projects, modeling software, and other activities.

• Developed excellent interpersonal communication.

• Performed advanced knowledge in SolidWorks.

Student Grader

Department of Electrical Engineering in the College of Engineering, University Park, PA

Skills & Ability:Software

• Microsoft office • SolidWorks • MATLAB • C++ Programming • HTML 5 • NI-Multisim • Labview

• AutoCAD • Arduino • Altium Designer • LATEX

Test Equipment

• Oscilloscopes • Network analyzer • Bode analyzer

Languages

• Mandarin • English

Conferences attend

The College of Engineering Design Showcase - December 2015

Title: GE project: A locomotive with the hydrogen power system.

Undergraduate Research Exhibition - April 2018

Title: Improvement of serpentine networks in crack resistance.

Electrical Engineering Project Fair - December 2018

Title: The design of a multi-sensing flexible system used for real-time monitoring